

MINISTRY OF EDUCATION
AND TRAINING

VIETNAM ACADEMY OF
SCIENCE AND TECHNOLOGY

GRADUATE UNIVERSITY OF SCIENCE AND TECHNOLOGY

PhD. Student. NGUYEN VAN TOAN

SYNTHESIS AND CHARACTERIZATION OF MULTIFUNCTIONAL
DRUG-CARRYING NANOGELS BASED ON CHITOSAN-PLURONIC
TOWARDS CANCER TREATMENT APPLICATIONS

Specialization: Organic Chemistry

Code: 9 44 01 14

SUMMARY OF DOCTORAL THESIS IN CHEMISTRY

Ho Chi Minh-2023

The thesis has been completed at: Graduate University of Science and Technology - Vietnam Academy of Science and Technology.

Supervisor 1: Assoc. Prof. Dr. Tran Ngoc Quyen

Supervisor 2: Dr. Luong Thi Bich

Reviewer 1:

Reviewer 2:

Reviewer 3:

The Doctoral thesis was defended at the Board of Examiners of Graduate University of Science and Technology-Vietnam Academy of Science and Technology at

The thesis can be referred at:

- Library of Graduate University of Science and Technology
- National Library of Vietnam

INTRODUCTION

1. The necessity of research

According to the biopharmaceutical classification system established by the US Food and Drug Administration (FDA), over 75% of active ingredients currently being researched in drug development exhibit poor solubility in physiological fluids. This hinders their absorption and delivery into the bloodstream. To address this issue, a promising approach involves incorporating these poorly soluble drugs into oil-based nano-core carriers, significantly enhancing their solubility. The hydrophilic nanoparticle's surface should readily disperse in aqueous environments, greatly improving the drug's solubility. Among various drug delivery systems, nanogel-based delivery systems are highly regarded due to their ability to enhance drug encapsulation efficiency through electrostatic and hydrophobic interactions. These systems also enable targeted delivery of anticancer drugs. Researchers have shown great interest in combining natural and synthetic polymers to develop nanogel drug delivery materials, as this approach capitalizes on the exceptional properties of each polymer. Chitosan, a natural polymer, is commonly used in biomedical materials for drug delivery due to its positive charged functional group ($-NH_2$), which can be easily modified or cross-linked with negatively charged molecules. Chitosan is non-toxic and exhibits good biocompatibility. Synthetic polymers such as amphoteric polymers based on poly(ethylene glycol) and poly(propylene glycol), such as Pluronic F68 and Pluronic F127, have been utilized in medical applications. Although Pluronic-grafted chitosan-based nanogels for drug delivery have been studied using Pluronic F127, there remain numerous unexplored Pluronic species. Furthermore, while chitosan or Pluronic alone has been studied in combination with target ligands like folic acid and biotin, the application of

Pluronic-grafted chitosan nanogels conjugated with these ligands has not yet been investigated.

In light of the aforementioned factors, we have undertaken the project titled "*Synthesis and characterization of multifunctional drug-carrying nanogels based on chitosan–Pluronic towards cancer treatment applications*".

2. Research objective

In this study, we aimed to prepare and characterize nanogels using chitosan grafted with various Pluronic types, ranging from hydrophobic to hydrophilic. Our objective was to determine the most effective Pluronic type for encapsulating curcumin in nanogels. Subsequently, we planned to develop nanogel drug delivery systems using chitosan-Pluronic conjugates, specifically the Pluronic type that showed the highest performance. These drug delivery systems would be designed to target breast cancer treatment by incorporating ligands such as folic acid and biotin, along with the drug paclitaxel.

3. Research content

1. Synthesis of chitosan drug delivery system grafted Pluronic with 4 types of Pluronic L61, P123, F127 and F68. Evaluation of chemical structure, physicochemical properties, ability to load and release curcumin, biocompatibility, ability to inhibit MCF-7 breast cancer cells of curcumin-carrying chitosan-Pluronic system.
2. Synthesis of chitosan-Pluronic drug delivery system conjugated with folic acid and biotin targeting agents. Evaluation of the chemical structure, physicochemical properties, loading and releasing capacity of paclitaxel, biocompatibility, ability to inhibit MCF-7 breast cancer cells of chitosan-Pluronic targeting system carrying paclitaxel.

CHAPTER 1. LITERATURE OVERVIEW

1.1. Chitosan-based drug delivery system

The combination of biocompatibility and biodegradability in chitosan (CS), along with the desirable properties of nanogels such as deformability, softness, large surface area, high loading capacity, and ease of stabilization, make CS-based nanogels a highly promising material for applications in drug delivery, cell culture, and therapy.

1.2. Pluronic-based drug delivery system

Polymer Pluronic®, approved by the FDA for pharmaceutical use, has undergone extensive research for various therapeutic applications. Due to their amphoteric properties, these copolymers possess surfactant characteristics, enabling interaction with hydrophobic surfaces and biofilms. When the concentration surpasses the critical micelle concentration (CMC), Pluronic micelles can spontaneously form, offering several advantageous qualities. The PPO blocks can effectively transport hydrophobic drugs, while the hydrophilic PEO chain provides stabilization and prevents rejection by the reticuloendothelial system. The hydrophilic segment of the micelle contributes to steric stability, resulting in prolonged circulation time in vivo, while the hydrophobic block copolymer exhibits high drug loading capacity and excellent compatibility. Additionally, the hydrophobic block of Pluronic enhances phagocytosis efficiency and facilitates drug absorption. Certain pluronics can also deplete intracellular adenosine triphosphate (ATP), inhibit the function of P-glycoprotein (P-gp), influence drug efflux and transport, and reverse multidrug resistance in tumors.

1.3. Pluronic grafted chitosan-based drug delivery system

The attachment of Pluronic monomer molecules to chitosan through conjugation enables them to form a cohesive structure, preventing dispersion at low concentrations. This conjugation plays a vital role in encapsulating hydrophobic drug molecules within the micelle core. Unlike other

polysaccharides like alginate and hyaluronic acid, chitosan conjugated with Pluronic yields micelles with enhanced strength and stability. This is due to the electrostatic interaction between the positively charged chitosan and the negatively charged Pluronic. Chitosan forms a hydrophobic outer shell within the micelle, which is primarily composed of the Pluronic PPO component.

CHAPTER 2. EXPERIENCE

2.1. Synthesis of chitosan – Pluronic (CS–Pluronic)

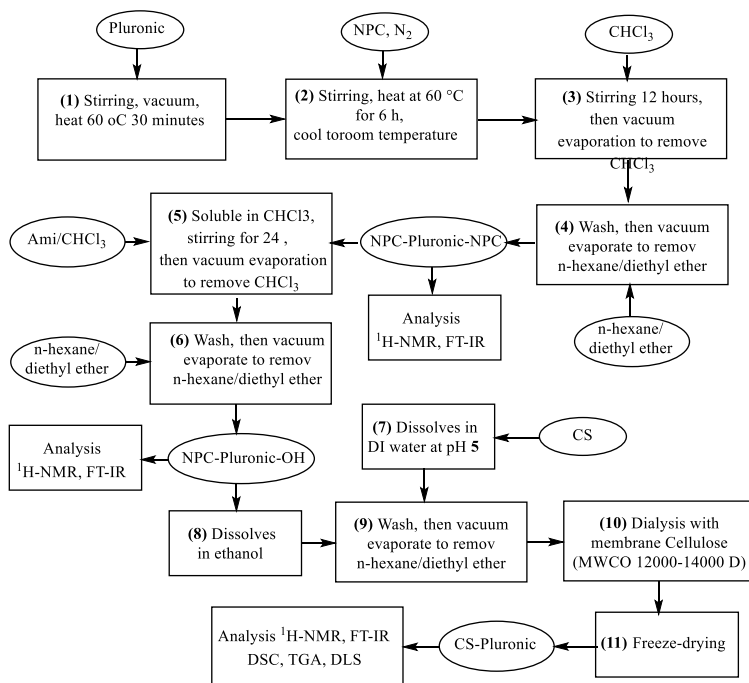


Figure 2. 1. Flowchart for the synthesis of CS-Pluronic.

The process of synthesizing CS-Pluronic, which involves the combination of chitosan with four different types of Pluronic (L61, P123, F127, and F68), can be divided into three stages. Firstly, the hydroxyl ends of Pluronic are activated using 4-Nitrophenyl chloroformate (NPC), resulting in the formation of NPC-Pluronic-NPC. Next, the NPC-Pluronic-NPC molecules undergo a substitution reaction, where a phenylcarbomate molecule is introduced at one end of the chain by a 3-Amine-1-propanol molecule. This step yields NPC-Pluronic-OH molecules. Finally, the NPC-Pluronic-OH molecules are grafted onto the chitosan chain, leading to the formation of CS-Pluronic. The synthesis process follows the flow chart depicted in Figure 2.1

2.2. Synthesis of folate-chitosan-Pluronic P123 (FA-CS-P123)

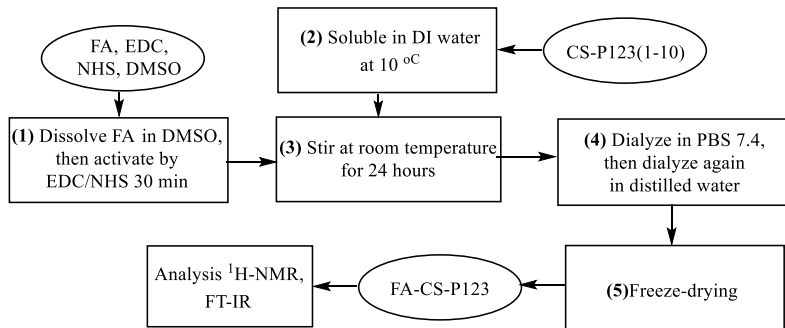


Figure 2. 2. Flowchart for the synthesis of FA-CS-P123.

FA-CS-P123 was synthesized by conjugating the FA molecule onto the chitosan chain of the CS-P123 molecule. The synthesis process is carried out according to the flow chart Figure 2.2

2.3. Synthesis of chitosan-Pluronic P123-folate (CS-P123-FA)

The production of CS-P123-FA involves three distinct phases. Firstly, the -NH₂ functional group is shielded and combined with EDA from the FA molecule, resulting in BOC-FA-NH₂. Next, the NPC group of the NPC-P123-NPC molecule is substituted to generate BOC-FA-P123-NPC. Lastly, BOC-FA-P123-NPC is attached to the CS chain, and the -BOC group is eliminated, yielding CS-P123-FA. The entire synthesis procedure adheres to the depicted flowchart in Figure 2.3.

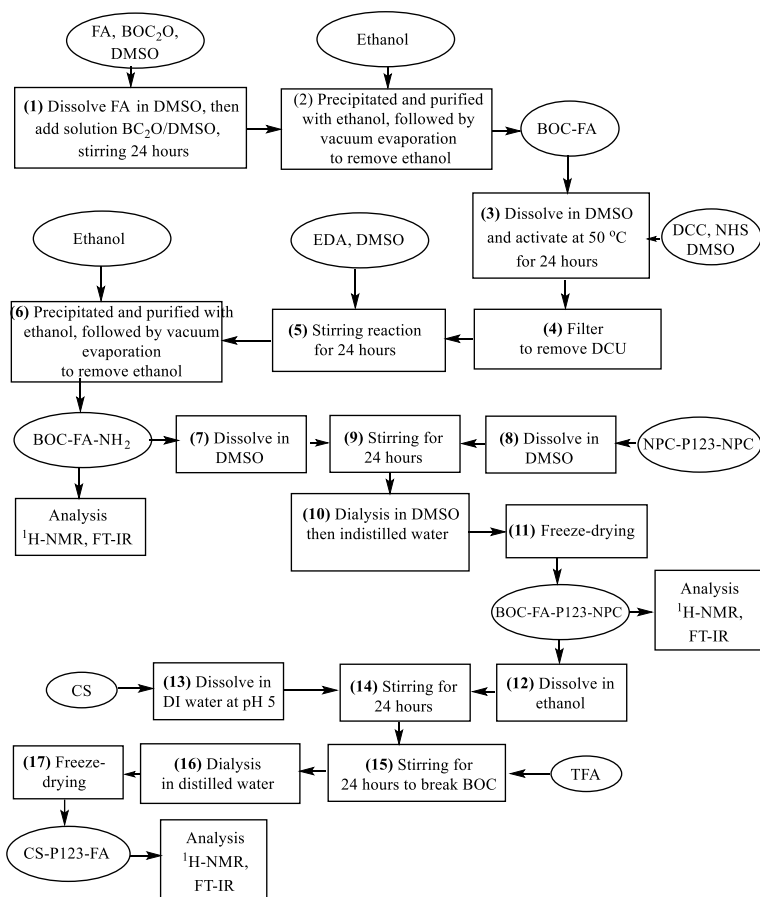


Figure 2. 3. Flowchart for the synthesis of CS-P123-FA.

2.4. Synthesis of chitosan–Pluronic P123–biotin (CS–P123–BIO)

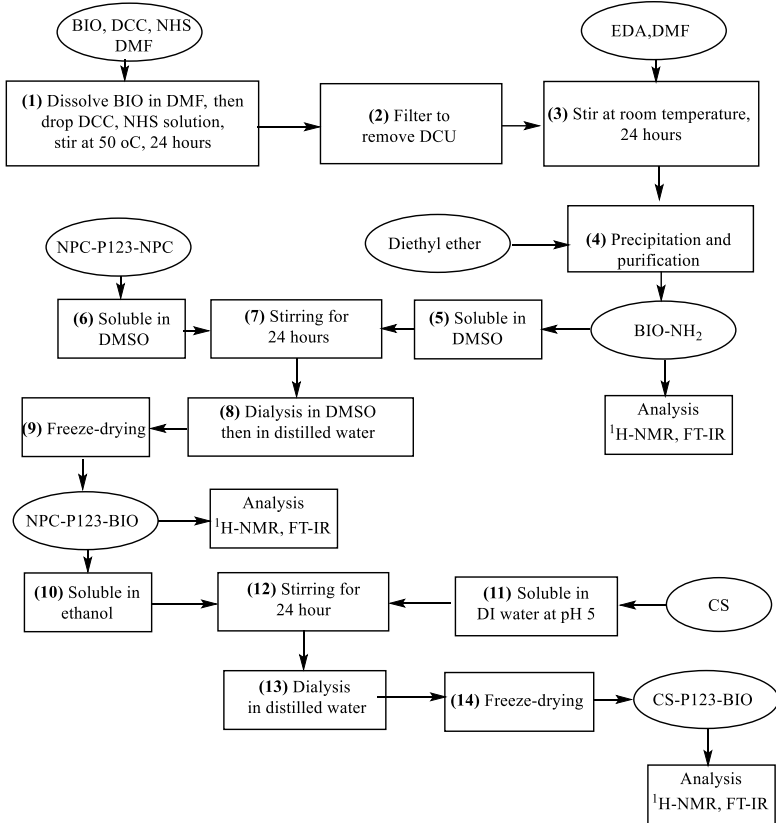


Figure 2. 4. Flowchart for the synthesis of CS–P123–BIO.

The synthesis of CS-P123-BIO involves three stages. In the first stage, BIO is combined with EDA to form BIO-NH₂. In the second stage, the NPC group in the molecule NPC-P123-NPC is replaced to obtain NPC-P123-BIO. Finally, NPC-P123-BIO is attached to the CS circuit to generate CS-P123-BIO. The entire synthesis process follows the flow chart depicted in Figure 2.4.

2.5. Determination of the critical micelle concentration (CMC) of nanogel

The iodine method was used in this study to determine the critical micelle concentration (CMC) value. In the presence of the hydrophobic environment provided by the Pluronic PPO blocks, soluble iodide ions interacted with excess KI in the solution, resulting in the conversion of I^{3-} to I_2 . When the CMC values were reached, the surfactants formed a fusion rather than individual micelles. As a result, there was no further conversion of I^{3-} to I_2 , which kept the absorption intensity of the mixed solution constant. Once micelles were formed, the converted I_2 molecules were trapped within the hydrophobic regions of the PPO blocks, leading to a significant increase in absorption intensity. The absorption intensity of I_2 was then plotted against the concentration degree of polymers.

2.6. Xác định khả năng nang hóa thuốc của nanogel

In this research, CUR served as a bioactive agent with hydrophobic properties, while PTX was utilized as an antineoplastic agent also possessing hydrophobic properties. Considering the properties of chitosan-Pluronic and the hydrophobic nature of the compounds, the thin film hydration technique emerged as the most suitable choice for encapsulating the drugs.

2.7. Investigation of drug release ability of nanogels

In this study, the nanogel system's ability to release drugs is commonly evaluated using the technique of membrane dialysis. The drug-loaded nanogel mixture is placed inside a dialysis membrane, which has pores larger than the size of the drug molecules but smaller than the polymer molecules. This ensures that only the drug molecules can pass through the membrane. The dialysis bag containing the nanogel mixture is then immersed in a release medium at different pH values, maintaining a temperature of 37 °C.

2.8. Evaluation of nanogel biocompatibility and cytotoxicity of drug-carrying nanogels

The compatibility of the nanogels with fibroblast cell lines and the toxicity of drug-loaded nanogels on the MCF-7 breast cancer cell line were evaluated using Sulforhodamine B (SRB) staining.

CHAPTER 3. RESULTS AND DISCUSSIONS

3.1 CS-Pluronic drug delivery system

3.1.1. Structural features

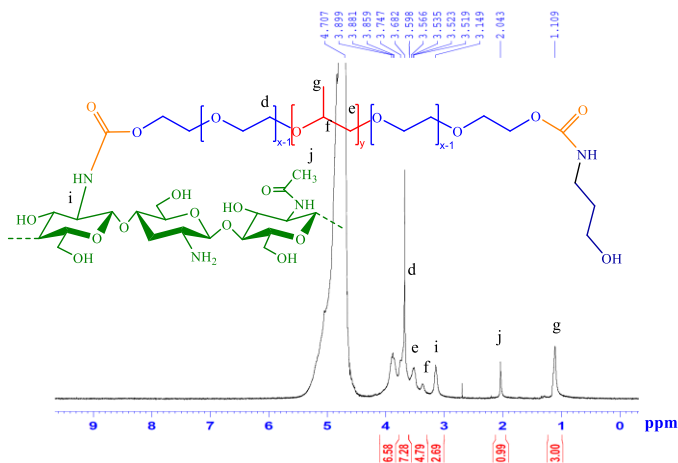


Figure 3. 1. The spectrum $^1\text{H-NMR}$ of CS-P123.

The nuclear magnetic resonance spectroscopy analysis (Figure 3.1) demonstrates distinct resonance peaks of protons in the Pluronic structure. These peaks are observed at $\delta \sim 3.7$ ppm (d), $\delta \sim 3.5$ ppm (e), $\delta \sim 3.3$ ppm (f), and $\delta \sim 1.1$ ppm (g). The presence of two peaks at $\delta \sim 3.0$ ppm (i) and $\delta \sim 2.0$ ppm (j) is attributed to protonation of the methylene group at positions C2 and methyl ($-\text{CH}_3$) in chitosan. Additionally, the absence of chemotactic signals of NPC at $\delta \sim 8.3$ ppm (a) and $\delta \sim 7.4$ ppm (b) suggests successful

grafting of Pluronic onto chitosan. Regarding the FT-IR spectra of CS–Pluronic nanogels, the characteristic oscillation peak of N–H binding of amine and amide II is weakened in CS–L61 and CS–P123, and completely lost in CS–F127 and CS–F68. Conversely, the oscillation peak characteristic of amide I is noticeably enhanced. This change is likely due to the conversion of the primary amine group ($-\text{NH}_2$) to an amide bond between chitosan and Pluronic (Figure 3.2).

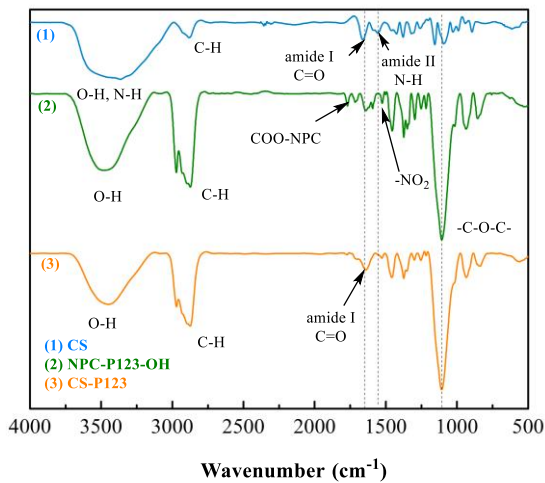


Figure 3. 2. The spectrum of FT-IR của CS (1), NPC-P123-OH (2) và CS-P123 (3).

The samples underwent scanning at temperatures ranging from 30 to 450 °C, with a heating rate of 10 °C/min. Figure 3.3 displays the results of the DSC analysis. Upon comparing the DSC heat histograms of CS–Pluronic and CS/Pluronic, a notable difference becomes apparent. In all CS–Pluronic heatmaps, there is an absence of exothermic peaks in the ~300 °C region, which are typically associated with the decomposition of amine units ($-\text{NH}_2$). On the contrary, the DSC heat chart of the CS/Pluronic mixture still exhibits exothermic peaks at specific temperatures: 284 °C (CS/L61), 306 °C

(CS/P123), 296 °C (CS/F127), and 297 °C (CS/F68). The reason behind the loss of the exothermic peak at ~300 °C in CS–Pluronic is the reaction between the $-\text{NH}_2$ groups of chitosan molecules and Pluronic molecules, leading to the formation of stable amide bonds.

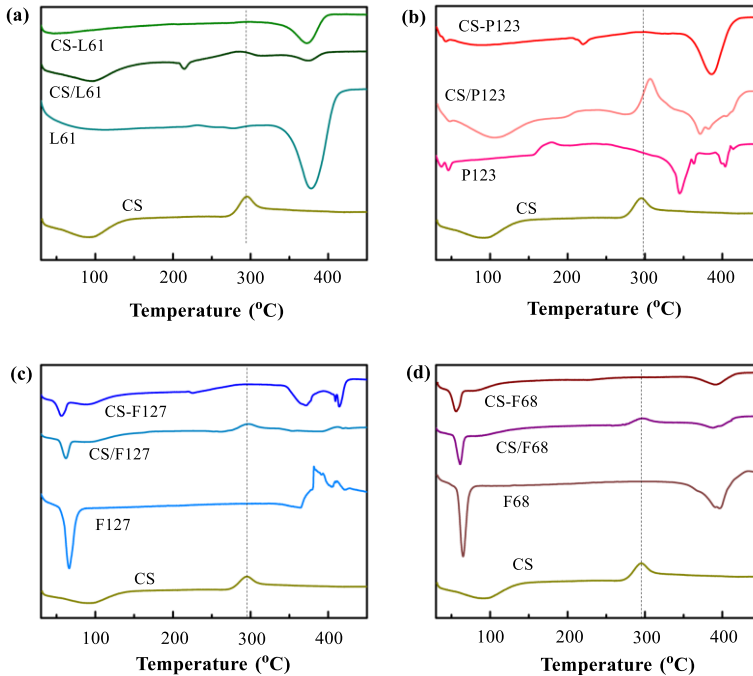


Figure 3. 3. DSC plot of CS, Pluronic types, CS–Pluronic types and CS/Pluronic physics mix. L61(a), P123(b), F127(c) and F68(d).

3.1.2. Determining the grafting ability of Pluronic onto CS circuit, the ability to encapsulate CUR and the characteristics of nanogel

Table 3.1 presents the calculation outcomes for the Pluronic content and grafting efficiency onto the chitosan circuit. The results indicate that the CS–L61 compound contains 64.38% of L61 with an efficiency of 82.02%. Similarly, the CS–LP123 compound contains 83.95% of P123 with a

grafting efficiency of 92.33%. The CS–F127 compound comprises 88.46% of F127 with a yield efficiency of 92.63%. Finally, the CS–F68 compound exhibits a content of 81.78% F68, along with an efficiency of 87.50%.

Table 3. 1. Reaction efficiency of Pluronic on chitosan.

Formulation	% <i>m</i> ₄₂₀ (CS)	% <i>m</i> ₄₂₀ (nanogel)	% <i>m</i> _{CS} (nanogel)	% <i>m</i> _{Pluronic} (nanogel)	% <i>H</i>
CS–L61	40.28	14.96	35.62	64.38	82.02
CS–P123	40.28	6.47	16.06	83.94	92.33
CS–F127	40.28	4.65	11.54	88.46	92.63
CS–F68	40.28	7.34	18.22	81.78	87.50

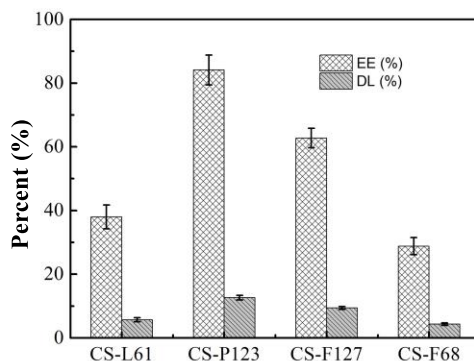


Figure 3. 4. CUR encapsulation efficiency of CS–Pluronic

The results of encapsulating CUR were assessed using two parameters, DL% and EE%, as depicted in Figure 3.4. The CS–L61, CS–P123, CS–F127, and CS–F68 nanogels exhibited DL% values of $5.70 \pm 0.65\%$, $12.62 \pm 0.71\%$, $9.41 \pm 0.46\%$, and $4.32 \pm 0.41\%$, respectively. The corresponding EE% values were $37.98 \pm 3.75\%$, $84.12 \pm 4.70\%$, $62.76 \pm 3.06\%$, and $28.82 \pm 2.71\%$.

Figure 3.5 displays the TEM findings for the spherical CS–Pluronic/CUR nanogels. The analysis reveals that the CS–Pluronic/CUR nanogel particles possess a kinetic diameter and zeta potential, indicating a size smaller than 200 nm and a positive charge. These characteristics make them suitable for utilization in cancer drug delivery applications, as summarized in Table 3.2.

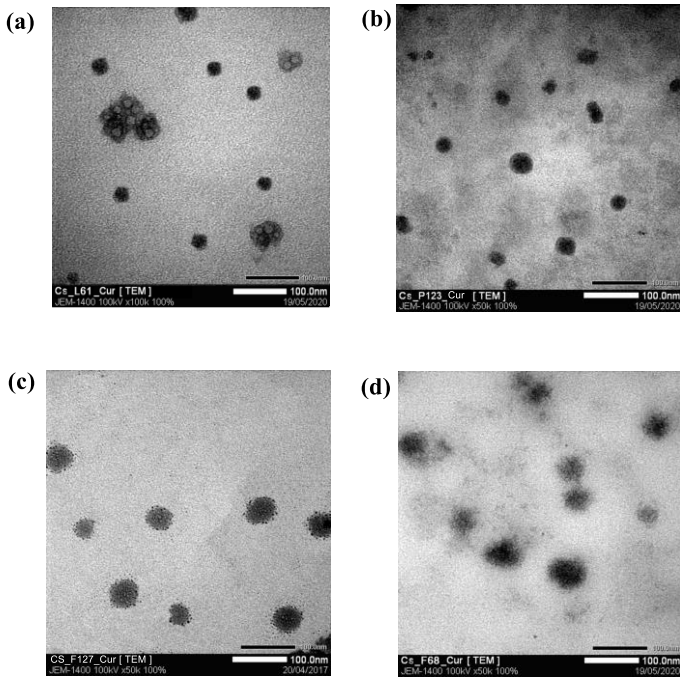


Figure 3. 5. TEM results of CS–L61/CUR (a), CS–P123/CUR (B), CS–F127/CUR (c) and CS–F68/CUR (d).

Table 3. 2. DLS results and zeta potential of CS–Pluronic/CUR . nanogels.

Formulation	DLS (nm)	Thé zeta (mV)
CS–L61/CUR	157 ± 5.6	99.6 ± 5.4
CS–P123CUR	77.6 ± 5.5	57.7 ± 3.7
CS–F127/CUR	86.7 ± 3.9	49.2 ± 4.9
CS–F68/CUR	147 ± 4.2	60.5 ± 5.1

3.1.3. The survey findings regarding the release capacity of CUR from CS–Pluronic/CUR nanogels.

Figure 3.6 illustrates the findings of the study examining the release capacity of CS-Pluronic nanogels for CUR. Generally, the CS-Pluronic/CUR nanogels effectively retained CUR at pH 7.4 but exhibited significant release at pH 5. Among the various nanogels, CS–P123 nanogels demonstrated the slowest release of CUR.

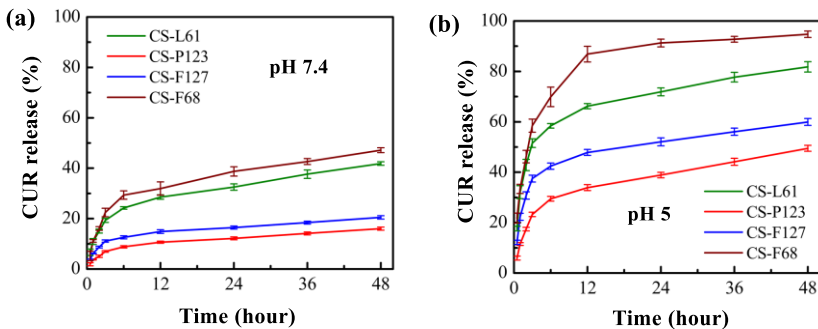


Figure 3. 6. Diagram depicting CUR release of CS–Pluronic nanogels at pH 7.4(a) and pH 5(b).

3.1.4. Evaluation of the storage stability of CUR-loaded nanogels after lyophilization

The nanogel's ability to retain drugs in micelle error during storage is assessed by evaluating the retention rate of CUR (DR%) within the nanogels. The storage ratio DR% values obtained after 6 months were 88.35 ± 3.95 (CS-L61/CUR), 97.91 ± 1.99 (CS-P123/CUR), 96.86 ± 4.23 (CS-F127/CUR), and 87.92 ± 8.92 (CS-F127/CUR). These results indicate that CS-P123 exhibits the highest hydrophobic drug storage capacity.

3.1.5. Biocompatibility testing of CS-Pluronic nanogel and breast cancer cytotoxicity of CS-Pluronic/CUR nanogels

After 48 hours of exposure, the viability of fibroblast cells incubated with CS-Pluronic nanogels at a concentration of $100 \mu\text{g/mL}$ was as follows: $74.78 \pm 4.87\%$ for CS-L61, $84.29 \pm 0.83\%$ for CS-P123, $86.20 \pm 0.96\%$ for CS-F127, and $91.87 \pm 1.44\%$ for CS-F68 (Figure 3.7). These results indicate that as the HLB value of Pluronics increases, such as L61 (HLB=3), P123 (HLB=8), F127 (HLB=22), and F68 (HLB=29), the biocompatibility of the high CS-Pluronic nanogel also increases.

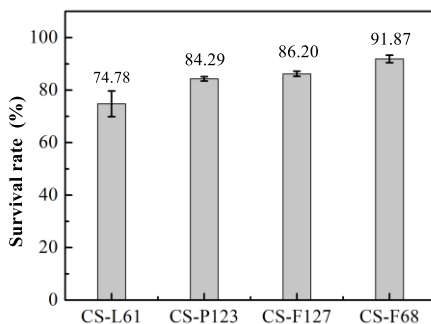


Figure 3. 7. Survival rate of fibroblast cells after 48 h incubation with CS-Pluronic nanogels.

Figure 3.8 illustrates the cytotoxicity results of MCF-7 cells. The IC₅₀ values are as follows: $16.15 \pm 0.62 \mu\text{M}$ for CUR, $4.72 \pm 0.46 \mu\text{M}$ for CS-L61/CUR, $13.09 \pm 0.38 \mu\text{M}$ for CS-P123/CUR, $11.48 \pm 0.63 \mu\text{M}$ for CS-F127/CUR,

and $11.20 \pm 0.40 \mu\text{M}$ for CS-F68/CUR. Consequently, the nanogel carrier significantly increased the toxicity of the nanogel in comparison to free CUR.

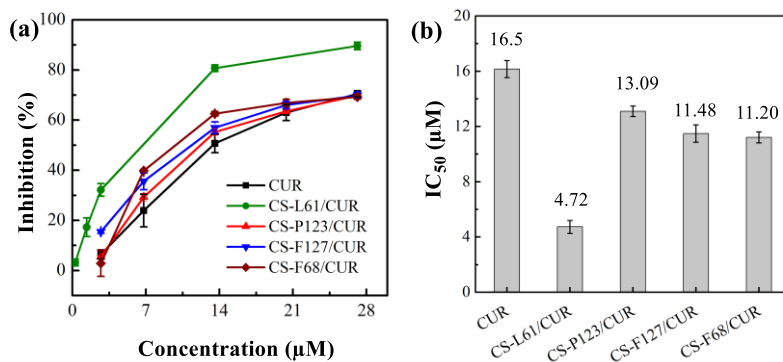


Figure 3. 8. Cytotoxicity results (a) and IC₅₀ values (b) in CUR.

3.2. Synthesis of targeted drug delivery systems with folate (FA) and biotin (BIO) ligands

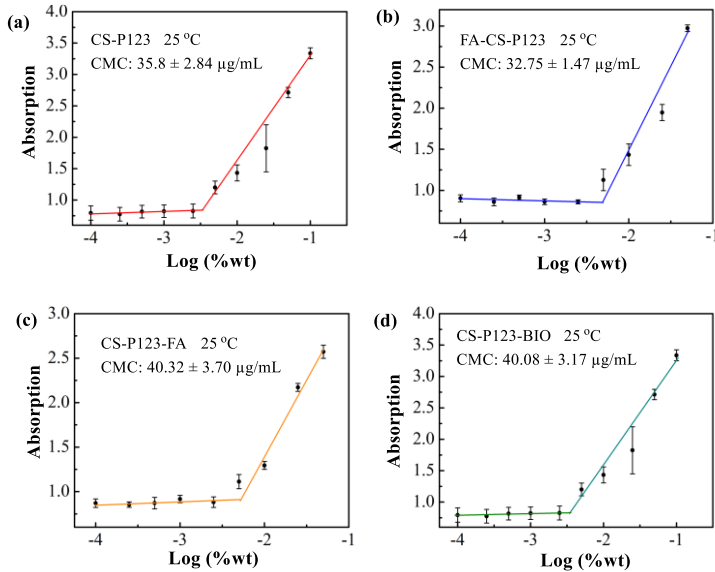
3.2.1. Structural features of FA-CS-P123, CS-P123-FA and CS-P123-BIO

The structural characteristics of the nanogel systems FA-CS-P123, CS-P123-FA, and CS-P123-BIO were investigated using ¹H-NMR and FT-IR spectroscopy. Analysis of the spectra confirmed the presence of FA and BIO ligands bound to the CS-P123 molecule.

3.2.2. Determination of CMC value, PTX encapsulation ability and nanogel characteristics.

The CMC measurements for CS-P123, FA-CS-P123, CS-P123-FA, and CS-P123-BIO are obtained from Figure 3.9. At 25 °C, the measured CMC values were as follows: $35.8 \pm 2.84 \mu\text{g/mL}$ for CS-P123, $32.75 \pm 1.47 \mu\text{g/mL}$ for FA-CS-P123, $40.32 \pm 3.70 \mu\text{g/mL}$ for CS-P123-FA, and $40.08 \pm 3.17 \mu\text{g/mL}$ for CS-P123-BIO. Comparatively, the CMC value of the nanogels

was lower than that of pure P123, which measured $89.64 \pm 16.37 \mu\text{g/mL}$. These results suggest that the nanogels exhibit greater thermodynamic stability than pure P123 micelles.



Hình 3. 9. Biểu đồ xác định giá trị CMC của CS-P123 (a), FA-CS-P123 (b), CS-P123-FA (c) và CS-P123-BIO (d).

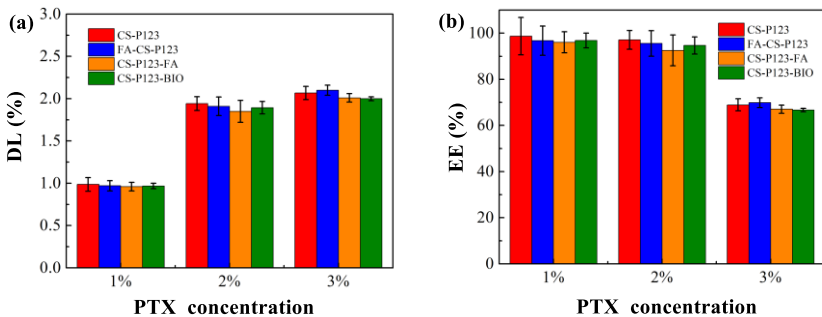


Figure 3. 10. Histograms represent the percentage of PTX (DL) (a) and PTX (EE) efficiency (b) carried in the nanogels.

Figure 3.10 illustrates the PTX encapsulation results of the nanogels. The nanogel formulations achieved the highest PTX encapsulation at a PTX concentration of 2%, with EE% values as follows: $93.00 \pm 7.32\%$ (CS-), $95.57 \pm 5.51\%$ (FA-CS-P123/PTX), $92.51 \pm 6.68\%$ (CS-P123-FA/PTX), and $87.17 \pm 7.96\%$ (CS-P123-BIO/PTX). There was no significant difference between 1% PTX and 2% PTX ($p > 0.05$), but a significant difference was observed between 2% PTX and 3% PTX ($p < 0.05$) in terms of EE%, indicating that using a PTX loading concentration of 2% minimizes PTX loss. Moreover, there was a significant difference between 1% PTX and 2% PTX ($p < 0.05$), but no significant difference between 2% PTX and 3% PTX ($p > 0.05$) in terms of DL%, suggesting that the nanogels have a maximum loading efficiency at approximately 2% PTX.

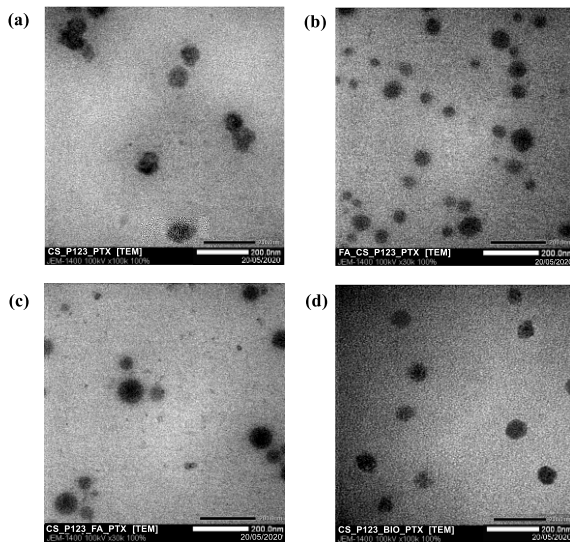


Figure 3. 11. TEM images of CS-P123/PTX (a), FA-CS-P123/PTX (b), CS-P123-FA/PTX (c) and CS-P123-BIO/PTX (d).

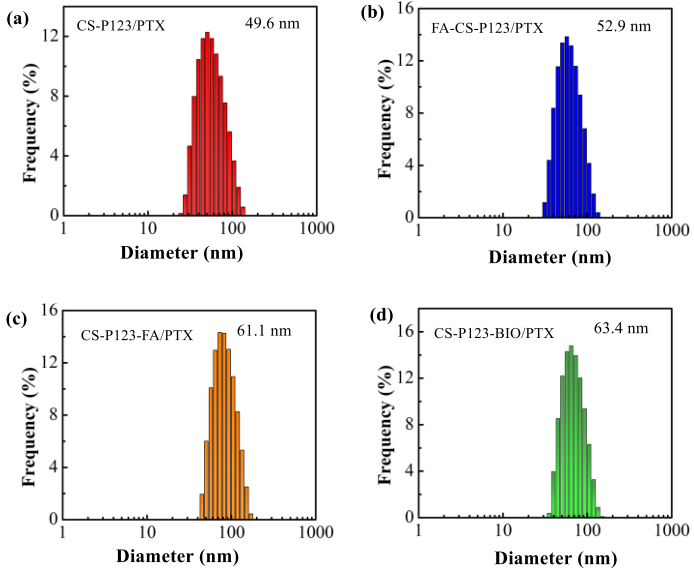


Figure 3. 12. DLS results of CS-P123/PTX (a), FA-CS-P123/PTX (b), CS-P123-FA/PTX (c) and CS-P123-BIO/PTX (d).

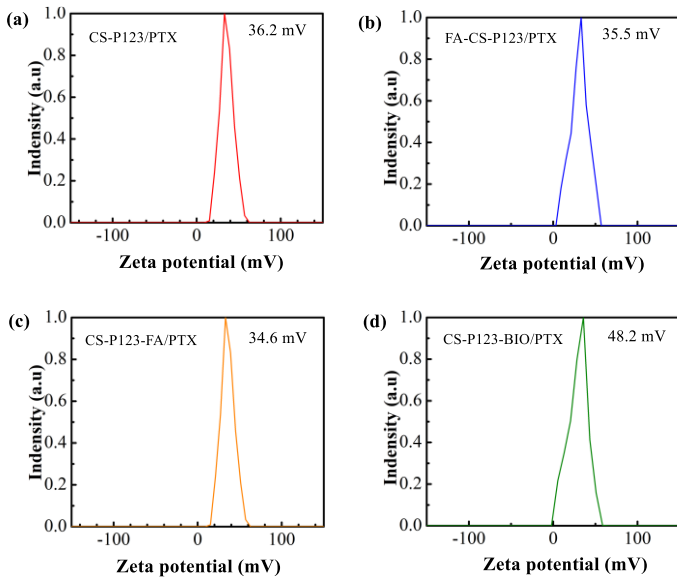


Figure 3. 13. Zeta potential results of CS-P123/PTX (a), FA-CS-P123/PTX (b), CS-P123-FA/PTX (c) and CS-P123-BIO/PTX (d).

Figure 3.11, Figure 3.12, and Figure 3.13 depict the TEM, DLS, and zeta potential findings of the PTX-carrying nanogels. According to the TEM and DLS analysis, the nanogels exhibit a spherical shape with the following kinetic diameters: 49.6 ± 1.1 nm (CS-P123/PTX), 52.90 ± 2.16 nm (FA-CS-P123/PTX), 61.13 ± 2.43 nm (CS-P123-FA/PTX), and 63.4 ± 0.6 nm (CS-P123-BIO/PTX). The recorded zeta potential values are as follows: 36.2 ± 1.6 mV (CS-P123/PTX), 35.5 ± 1.3 mV (FA-CS-P123/PTX), 34.6 ± 1.0 mV (CS-P123-FA/PTX), and 48.2 ± 1.0 mV (CS-P123-BIO/PTX).

3.2.3. The survey findings regarding the release capacity of PTX from nanogels.

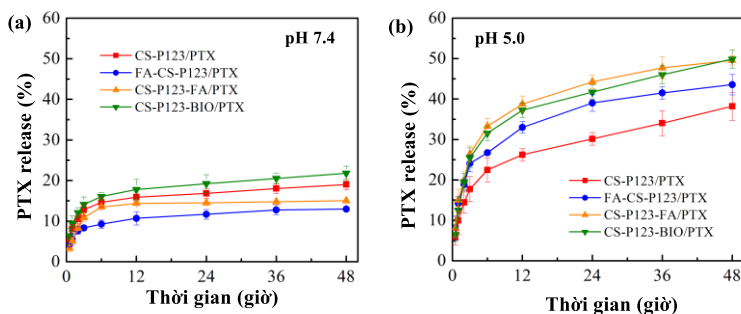


Figure 3. 14. The graph depicts the PTX release of the nanogels at pH 7.4 (a) and pH 5.0 (b).

The release of PTX from FA-CS-P123/PTX and CS-P123-FA/PTX nanogels was assessed in two different environments: physiological conditions (pH 7.4) and within the tumor (pH 5), as depicted in Figure 3.14. The findings demonstrated that, at pH 7.4, the cumulative percentage of PTX released from the nanogels was 19.02% (CS-P123/PTX), 12.96% (FA-CS-P123/PTX), and 15.04% (CS-P123-FA/PTX), respectively. Furthermore, the release percentages were 21.78% (CS-P123-BIO/PTX) and 48.21% (CS-P123/PTX) after 48 hours. However, at pH 5.0, the PTX release from the

nanogels after 48 hours significantly increased, reaching 38.21% (CS-P123/PTX), 43.56% (FA-CS-P123/PTX), and 49.86% (CS-P123-FA/PTX), respectively (CS-P123-BIO/PTX).

3.3.4. Evaluation of the storage stability of PTX-loaded nanogels after lyophilization

The nanogels containing PTX were examined for stability over a period of six months at room temperature. The results indicate a minor decline in EE% and DL%, along with a slight rise in the size of the micelles (DLS) and zeta potential, which signifies stability. Furthermore, the nanogels exhibited a remarkable retention rate of PTX (DR%) exceeding 95%.

3.3.5. Biocompatibility testing of nanogel and breast cancer cytotoxicity of PTX-loaded nanogels

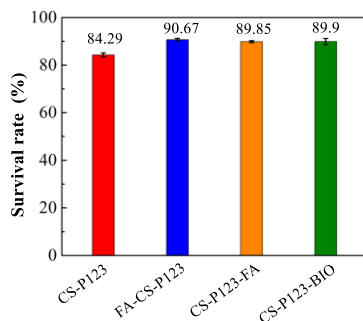


Figure 3. 15. Survival rate of fibroblast cells after tumor with nanogel at concentration of 100 g/mL after 48 hours.

Figure 3.15 illustrates the outcomes of the biocompatibility test conducted on fibroblast cells. After a 48-hour exposure, the viability percentages of fibroblast cells incubated with nanogels were as follows: $84.29 \pm 0.83\%$ for CS-P123, $90.67 \pm 0.55\%$ for FA-CS-P123, $89.86 \pm 0.42\%$ for CS-P123-FA, and $89.90 \pm 1.26\%$ for CS-P123-BIO, all at a concentration of 100 $\mu\text{g/mL}$. The findings demonstrate that nanogels carrying targeted

ligands exhibited a lower capacity to impede fibroblast cell growth compared to those without ligands (CS–P123).

Figure 3.16 displays the cytotoxicity results of MCF-7 cells. The IC_{50} values obtained were as follows: 8.19 ± 1.17 nM (free PTX), 18.08 ± 0.55 nM (CS–P123/PTX), 8.31 ± 1.99 nM (FA–CS–P123/PTX), 3.27 ± 0.35 nM (CS–P123–FA/PTX), and 4.80 ± 0.46 nM (CS–P123–BIO/PTX). The findings indicate that nanogels carrying FA or BIO target ligands exhibit greater efficacy in killing MCF-7 cells compared to ligand-free nanogels (CS–P123) and free PTX. However, the ability of FA–CS–P123/PTX to kill MCF-7 cells is lower than that of CS–P123–FA/PTX due to the relatively lower FA content in FA–CS–P123 compared to CS–P123–FA.

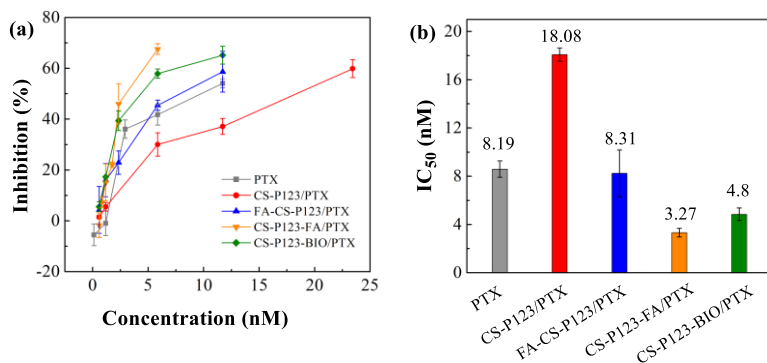


Figure 3. 16. Cytotoxicity results (a) and IC_{50} values (b) of free PTX and PTX-carrying nanogels.

CONCLUSIONS AND RECOMMENDATIONS

CONCLUSIONS

The thesis achieved several notable outcomes, which can be summarized as follows:

1. We successfully developed a drug delivery system using CS–Pluronic nanogels, incorporating four different types of Pluronic polymers: L61,

P123, F127, and F68. The synthesis was confirmed through various spectral analyses, including $^1\text{H-NMR}$, FT-IR, TGA, and DSC. By evaluating the relationship between DL (%), CMC, and HLB values of each Pluronic type, we found that the CS-P123 nanogel exhibited the highest drug loading (DL %), followed by CS-F127, CS-L61, and CS-F68. The CMC values followed a similar trend, with CS-P123 having the lowest CMC, followed by CS-F127, CS-L61, and CS-F68. Regarding the HLB values, L61 had the lowest value, followed by P123, F127, and F68. Therefore, the encapsulation ability of CS-Pluronic nanogels for the drug CUR depended on both the CMC values of CS-Pluronic and the specific Pluronic polymer used, but not on the HLB value of the precursor Pluronic.

2. The CS-P123 drug delivery system was successfully synthesized using targeted agents FA and BIO. Extensive analysis, including $^1\text{H-NMR}$, FT-IR, TGA, DSC, TEM, and DLS, was conducted to determine the chemical structure, CMC value, PTX encapsulation ability, morphological characteristics, size, and charge of the nanogels. The results revealed that the PTX encapsulation ability of the nanogels was consistently high, reaching an optimal level of 2% PTX. Moreover, the nanogels exhibited suitable size for efficient drug delivery. In vitro tests demonstrated the strong release of PTX by the nanogel in an acidic environment while maintaining stability in the body's physiological conditions. A novel approach was implemented by incorporating the FA-targeted ligand conjugation on the Pluronic P123 circuit of the CS-P123-FA system, which had not been previously studied. A comparison was made with the design of FA-ligand conjugation on the chitosan circuit of the FA-CS-P123 system. The CS-P123-FA system exhibited a higher FA content (0.71%) compared to the FA-CS-P123 system (0.31%), enabling effective targeted interaction with breast cancer cells (MCF-7). This was validated through fluorescence imaging and the enhanced ability of CS-P123-FA/PTX ($\text{IC}_{50}= 3.27 \text{ nM}$) to induce cell death

in MCF-7 cells as compared to FA-CS-P123/PTX (IC_{50} = 8.31 nM). Based on these findings, the BIO target ligand was considered as an alternative conjugate design option with the Pluronic P123 circuit in the CS-P123-BIO system to evaluate its effectiveness in comparison to FA. The evaluation of PTX's ability to kill MCF-7 cells using CS-P123-BIO/PTX nanogel (IC_{50} = 4.8 nM) confirmed that BIO is a viable ligand replacement for FA in the design of targeted drug delivery for cell division.

LIST OF PUBLICATIONS

1. Lyna Pham, Le Hang Dang, Minh Dung Truong, Thi Hiep Nguyen, Ly Le, Van Thu Le, Nguyen Dang Nam, Long Giang Bach, **Van Toan Nguyen**, Ngoc Quyen Tran, A dual synergistic of curcumin and gelatin on thermal-responsive hydrogel based on Chitosan-P123 in wound healing application, *Biomedicine & Pharmacotherapy*, **2019**, *117*, 109183. IF: 7.419, Q1.
2. **Van Toan Nguyen**, Phuong Doan, Dinh Trung Nguyen, Van-Dat Doan, Tan Phat Dao, Vitalii Plavskii, Bich Tram Nguyen, Ngoc Quyen Tran, Effect of targeting ligand designation of self-assembly chitosan-poloxamer nanogels loaded Paclitaxel on inhibiting MCF-7 cancer cell growth. *Journal of Biomaterials Science, Polymer Edition*, **2021**, *33(4)*, 426-442. IF: 3.517, Q2.
3. **Van Toan Nguyen**, Quoc Trung Nguyen, Ngoc Thach Pham, Dinh Trung Nguyen, Tri Nhut Pham, Ngoc Quyen Tran, An in vitro investigation into targeted paclitaxel delivery nanomaterials based on CS-Plu P123-biotin copolymer for inhibiting human breast cancer cells. *Journal of Drug Delivery Science and Technology*, **2021**, *66*, 102807. IF: 5.062, Q1.